nature physics

ARTICLES

PUBLISHED ONLINE: 24 JANUARY 2010 | DOI: 10.1038/NPHYS1510

Turbulent inward pinch of plasma confined by a levitated dipole magnet

A. C. Boxer[1], R. Bergmann[1], J. L. Ellsworth[1], D. T. Garnier[2], J. Kesner[1], M. E. Mauel[2]* and P. Woskov[1]

The rearrangement of plasma as a result of turbulence is among the most important processes that occur in planetary magnetospheres and in experiments used for fusion energy research. Remarkably, fluctuations that occur in active magnetospheres drive particles inward and create centrally peaked profiles. Until now, the strong peaking seen in space has been undetectable in the laboratory because the loss of particles along the magnetic field is faster than the net driven flow across the magnetic field. Here, we report the first laboratory measurements in which a strong superconducting magnet is levitated and used to confine high-temperature plasma in a configuration that resembles planetary magnetospheres. Levitation eliminates field-aligned particle loss, and the central plasma density increases markedly. The build-up of density characterizes a sustained turbulent pinch and is equal to the rate predicted from measured electric-field fluctuations. Our observations show that dynamic principles describing magnetospheric plasma are relevant to plasma confined by a levitated dipole.

Since the discovery of the Earth's radiation belts more than fifty years ago, observations of energetic particles trapped in the Earth's dipole magnetic field have illustrated a remarkable and non-intuitive process: random, low-frequency fluctuations caused by solar activity create diffusion that drives particles inward towards the Earth and increases particle density[1–4]. Instead of flattening density gradients, diffusion causes particles trapped in a magnetic dipole to become peaked. The central peaking of particle density—occurring in opposition to the usual direction of diffusion—characterizes a 'turbulent pinch'. In strongly magnetized plasma, charged particles have gyro-radii very much smaller than the size of the plasma[5], and plasma motion along the magnetic field is fundamentally different from motion across the field[6]. Low-frequency fluctuations cause the random radial motion of entire populations of particles contained within field-aligned tubes of magnetic flux, and this motion links the geometry of the magnetic field to the particle density profile. For the Earth's magnetosphere, random fluctuations of the solar wind cause radial diffusion that equalizes the number of particles within tubes of equal magnetic flux (and not within equivalent volumes of space), and this causes the density of inward diffusing energetic particles to increase markedly[3,7–9]. Although laboratory experiments have observed space-related plasma phenomena before[10], the study of the cross-field transport of plasma trapped in a dipole magnetic field has been limited to fast outward diffusion driven by internal instabilities[11,12]. Until now, equilibrium profiles that develop over long timescales by cross-field transport were unobservable in the laboratory because the losses of particles along field lines to the magnetic poles prevented the establishment of centrally peaked profiles from inward radial diffusion.

We report results from a new experiment, using a levitated superconducting current ring, that demonstrates that the cross-field processes and profiles that characterize active planetary magnetospheres can also be made to appear in the laboratory. In particular, we present the first laboratory measurements of a strong turbulent particle pinch in a dipole-confined plasma that results from the random, self-generated electric-field fluctuations sustained by plasma heating. Although the inward turbulent pinch has been observed before in tokamak devices used for fusion energy research[13–17], turbulent transport of plasma in a dipole field results in pronounced central peaking and a turbulent pinch that is easily detected. Indeed, the dipole magnetic field from either a current ring or a magnetized planet is the simplest field that confines charged particles, making our observations of plasma dynamics relevant to the study of planetary magnetospheres[18,19], turbulence in magnetized plasma[20], and magnetic confinement of high-temperature plasma for thermonuclear fusion energy[21].

The levitated dipole experiment (LDX) was built so that magnetic field lines pass through the current ring and produce a large volume of closed field lines that do not strike any surface of the laboratory device. When the dipole magnet is levitated, high-speed measurements of the plasma with a four-chord microwave interferometer[22] show the development of centrally peaked density profiles from inward diffusion that resemble periods of strong convection in active magnetospheres[23]. The density profile is characterized by a nearly equal number of particles within tubes of equal magnetic flux, which is the condition for marginal stability of the centrifugal interchange instability[12,24] and also the relaxed state of diffusion induced by random low-frequency fluctuations of electric and magnetic fields[1–3]. In comparison, when the dipole magnet is mechanically suspended, the density profile is relatively uniform and shows no evidence of central peaking. Photographs of the light emitted from neutral gas show that the ionization source of plasma particles is gas entering the plasma from the outer edge. We therefore conclude that the large increase of central density that occurs when the dipole is magnetically levitated is the result of an inward particle pinch that is driven by a cross-field transport process that is only observed in the absence of field-aligned losses.

Our observation of a centrally peaked density profile not only extends previous observations of high-pressure plasma confinement by a dipole magnet[25] but also experimentally validates a central principle of a potentially attractive device in which to produce thermonuclear fusion power[26]. A dipole fusion power source requires a high-pressure, centrally peaked plasma profile

[1]Plasma Science and Fusion Center, Massachusetts Institute of Technology, Cambridge, Massachusetts 02139, USA, [2]Department of Applied Physics and Applied Mathematics, Columbia University, New York, New York 10027, USA. *e-mail: mauel@columbia.edu.

© 2010 Macmillan Publishers Limited. All rights reserved.

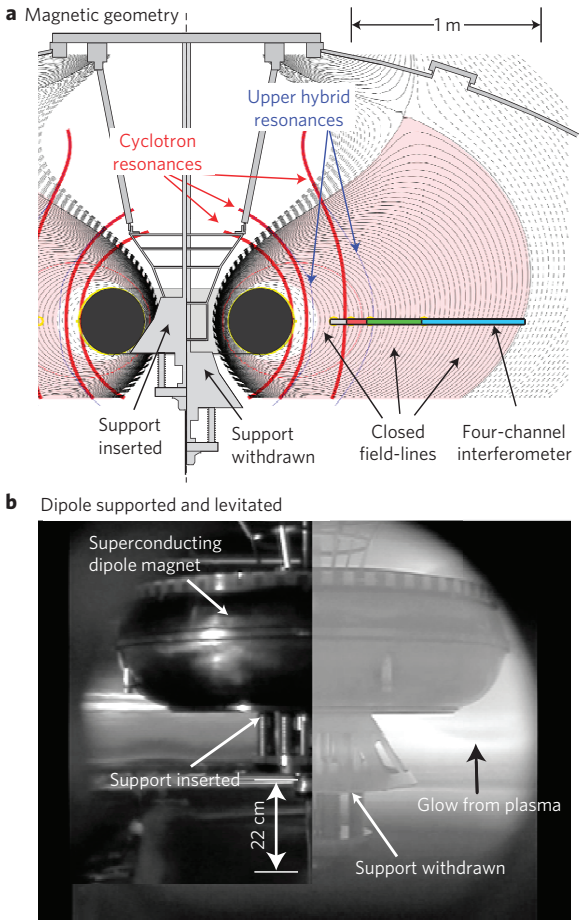

Figure 1 | Magnetic geometry of the superconducting dipole and photograph of lifting apparatus when inserted and withdrawn. a, The magnetic field lines and microwave resonances are unchanged during experiments with either mechanical support or magnetic levitation. However, during levitation, field lines that cross the equator between 0.68 and 1.71 m do not contact material surfaces. The four-channel interferometer array passes through the plasma and measures the integral of the plasma density along each ray path. **b**, During levitation, the lifting support is withdrawn 0.22 m from the dipole.

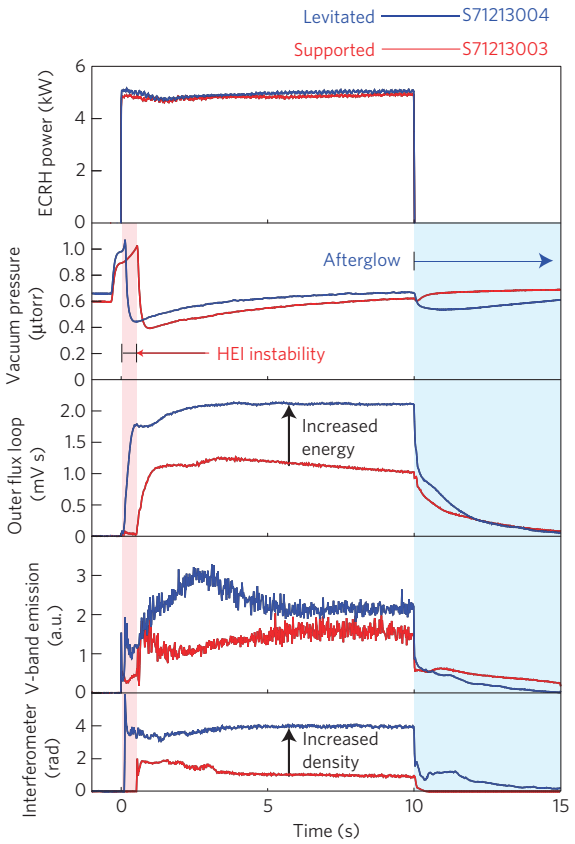

Figure 2 | Comparison of two nearly identical plasma discharges produced with a supported and levitated dipole magnet. Recorded measurements with a supported dipole are shown in red and with a levitated dipole in blue. 5 kW of microwave heating, with equal power from 2.45- and 6.4-GHz sources, was applied for 10 s. Levitation causes three changes: (1) a short period of HEI instability is eliminated; (2) the plasma ring current doubles as indicated by increased flux measured by 5-m-diameter flux loop; and (3) the central line density increases by more than a factor of two. The level of cyclotron radiation and the long-time behaviour of the 'afterglow' changes very little.

because it would use a fusion fuel cycle based on deuterium and helium-3 (ref. 27) instead of the deuterium and tritium fuel proposed for tokamak devices[21]. Although fusion with helium-3 requires a higher plasma temperature and confinement, it simplifies some of the technologies needed for fusion because there would be no need to breed tritium from lithium nor a need to engineer materials that resist damage caused by the very energetic neutrons from fusion with tritium[28,29].

Plasma confined by a levitated dipole magnet

Figure 1 shows a cross-sectional view of the magnetic geometry of the LDX device as well as the radial locations of the four chords of the interferometer array and the locations of axisymmetric surfaces where injected microwaves resonate with and heat plasma electrons. A toroidal region of closed magnetic field lines encircles the dipole magnet and extends from an equatorial radius of 0.68 m outward to 1.71 m. Inside this region, magnetic field lines conduct plasma particles to the dipole magnet; outside, magnetic field lines strike the vacuum vessel. The outer boundary between closed and open field lines is a surface where field lines pass through a field null formed by the cancellation of the dipole field with an opposing field from the upper levitation coil. Plasma is heated and sustained by injecting microwave power (as described in the Supplementary Information). Microwave heating is coupled to plasma on all field lines; however, a small number of electrons, which are magnetically trapped on field lines with a cyclotron resonance near the equatorial plane of the dipole, are heated to very high, quasi-relativistic energies near 150 keV. These hot electrons are very well confined by the dipole field, whether it is levitated or supported, and resemble trapped radiation belt particles in the magnetosphere[3]. As shown in Fig. 1a, the four interferometer chords pass through the outer plasma and reach an inner radius at 0.77, 0.86, 0.96 and 1.25 m, respectively. The measured phase shift along each chord is proportional to the integral of the density along the ray path between the interferometer transmitting and receiving horns. Taken together, the four interferometer chords constrain the shape of the radial density profile. For example, when the line-integrated density along the inner cord (reaching 0.77 m) significantly exceeds the line-integrated density along the next cord (reaching 0.86 m), then the inner density must exceed the outer density.

Magnetic levitation profoundly changes the properties of plasma created with nearly equivalent heating power and neutral gas fuelling. Figure 2 compares two discharges, levitated and supported. A total of 5 kW of microwave power was injected for 10 s. Just before the injection of microwaves, deuterium gas was injected into the vacuum vessel, reaching a pressure of approximately

© 2010 Macmillan Publishers Limited. All rights reserved.

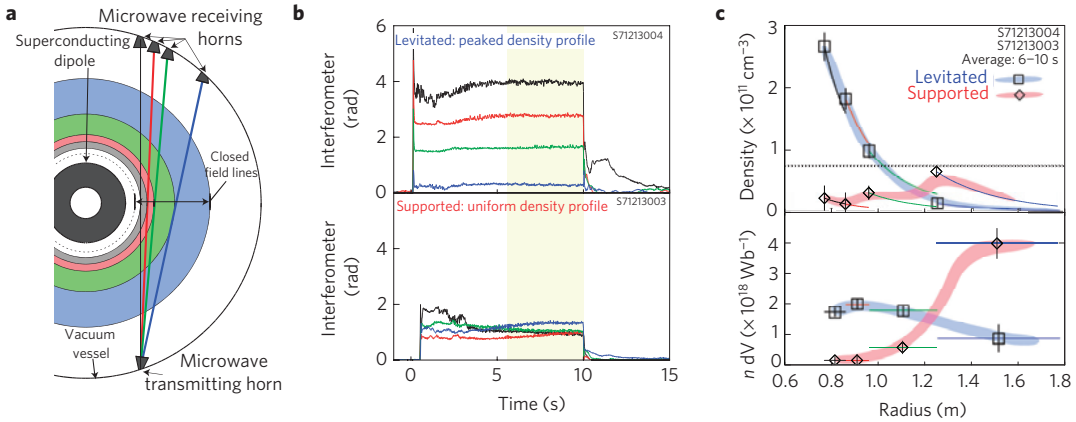

Figure 3 | Measurements using the four-channel interferometer array show that levitation results in a highly peaked plasma density profile. a, The four interferometer chords pass through different radial regions of the plasma. **b**, When the dipole is supported, the four microwave interferometer chords show similar line densities. In contrast, when levitated, the line density measurements increase for the central chords and decrease in the outer region. **c**, Reconstructed plasma density (shown in top panel, error bars representing standard deviation from the time average) increases by nearly an order of magnitude near $R \sim 0.8$ m. The particle number per unit magnetic flux, $\langle n \rangle dV$ (shown in bottom panel), is hollow with a supported dipole and relatively uniform when the dipole is levitated.

1 μtorr. When the dipole is supported, the discharge behaviour and parameters are like those previously reported[25] except, in these discharges, the levitation coil was energized even when the dipole was mechanically supported so that the geometry of the magnetic flux tubes is the same during supported and levitated conditions. For the discharge in Fig. 2 with a supported dipole, intense hot electron interchange (HEI) instabilities (see Supplementary Information) were excited during the first 0.5 s of the heating pulse. After the HEI stabilizes, the plasma density rapidly increases and the plasma diamagnetic current, or the 'plasma ring current', also increases, but more gradually. The plasma diamagnetic current density and the plasma pressure gradient are related by the condition for magnetohydrodynamic equilibrium (see Supplementary Information). For a dipole magnetic field, including the Earth's magnetosphere, the magnetic field (or flux) resulting from the ring current is proportional to the plasma stored energy. For LDX, the ratio of the total plasma stored energy to the outer-flux-loop measurement is approximately 90 J per mV s^{-1} (as shown in Supplementary Fig. S3). When the microwave heating is switched off, the plasma density decays rapidly while the plasma diamagnetic current decays over several seconds, indicative of the long confinement time of the hot electrons. In contrast, when the dipole is levitated, HEI instabilities are rarely observed, and both the plasma stored energy (as measured by the change of outer magnetic flux) and the line density (as measured by the inner-most interferometer chord) increase by at least a factor of two.

Levitation improves magnetic plasma confinement, but the most pronounced change from levitation is the change in the plasma's density profile. Figure 3b shows the four measured interferometer chords for the two discharges shown in Fig. 2. When the dipole is levitated, the measured line densities from the four chords increase as the tangency radius moves inward from 1.25 to 0.77 m. In contrast, all four chords show nearly the same line density when the dipole is supported. These measurements can be used to estimate the plasma radial profile through a model-dependent inverse integral calculation. Figure 3c shows one estimate of the density profile based on a model motivated by the dynamics of magnetospheric interchange convection. The particle content within tubes of given magnetic flux, N, is assumed to be constant within the four annular sections traced by the interferometer chords. (These regions are shaded with different colours in Fig. 3a.) The density is taken to be uniform within any flux tube, so the equatorial density is related to the particle number as $\langle n \rangle = N/\delta V$, where the differential volume of a tube of magnetic flux is $\delta V = \oint \mathrm{d}s/B$. For the dipole field, the flux-tube volume increases rapidly with the equatorial radius, $\delta V \sim L^4$. Figure 3c shows the computed density profiles, averaged over the interval from 6 to 10 s. When the dipole is supported, $\langle n \rangle$ is approximately uniform, or a slightly hollow function of radius, and N peaks on the outside. When the dipole is levitated, $\langle n \rangle \propto 1/\delta V$, implying that N is nearly uniform. The density on the inside of the closed field-line region increases by more than an order of magnitude, whereas the density decreases in the outer region. We find the shape of the density profile varies with gas pressure and heating power, but it is always strongly peaked during levitation and nearly uniform, or hollow, with a supported dipole.

Measurement of the turbulent pinch

The strongly peaked density profiles are established within 25 ms. Figure 4 shows measurements from comparable supported and levitated discharges produced with a short, 0.5 s, 11 kW heating pulse. The deuterium pressure was adjusted to 4 μtorr, which stabilized the HEI instability at the onset of heating. For the first 3 ms, the plasma density build-up does not depend on whether the dipole is supported or levitated. The density profile is uniform or slightly hollow, as was the case in Fig. 3c. However, after this initial increase, when the dipole is levitated, the density continues to increase for a further 20–30 ms and becomes highly peaked. Figure 4b shows photographs of the plasma light for these two discharges taken at the same time. The light emission is hollow during levitation and approximately uniform with a supported dipole. As light emission is indicative of ionization, the photograph implies the peaked density profile that appears during levitation must be due to a cross-field plasma transport process and not caused by a more centrally located ionization source. Figure 4a also shows the time evolutions of the outer flux loop, the cyclotron emission from the hot electrons at 137 GHz and the root-mean-squared (r.m.s.) fluctuations of the edge azimuthal electric field measured with an array of floating potential probes.

The timescale for the inward turbulent pinch caused by random fluctuations in the Earth's cross-tail electric field driven by the solar wind was calculated in ref. 2 for particles trapped in the magnetosphere. When the fluctuations have frequencies much less than the ion cyclotron frequency, the fluctuating azimuthal electric field, E_φ, induces random radial motion of plasma that is both hydromagnetic and interchange-like[6]. The particles contained

© 2010 Macmillan Publishers Limited. All rights reserved.

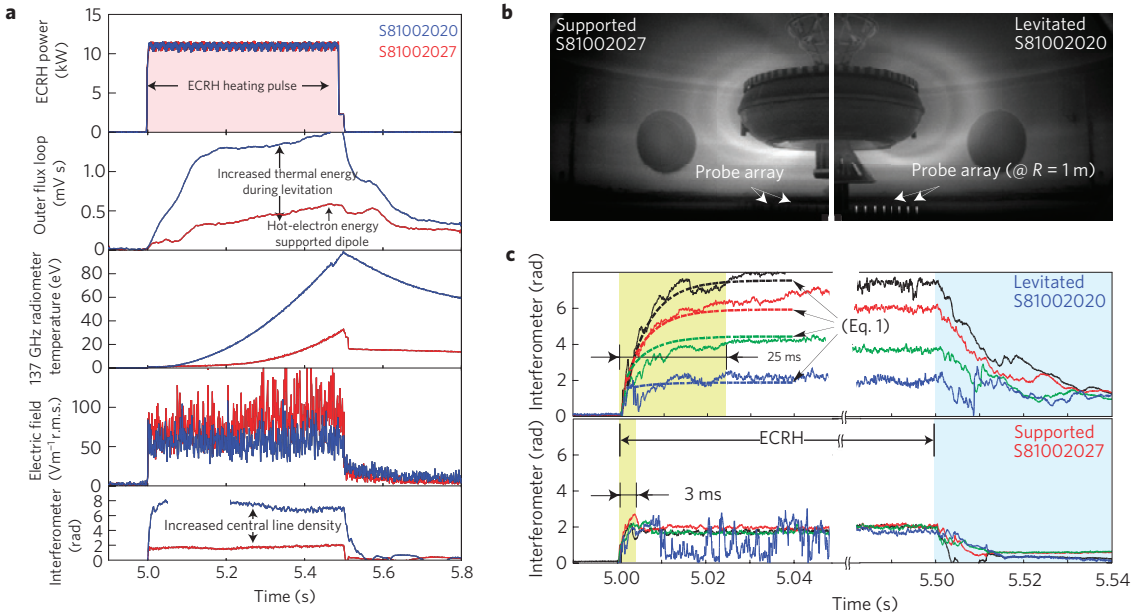

Figure 4 | Measurement of the time required to establish the centrally peaked profile is used to determine the rate of the inward particle pinch. a, Two plasma discharges were created under nearly identical conditions using short, half-second heating pulses 2.5 kW of 2.45 GHz and 9.5 kW of 10.5 GHz microwaves. Plasma measurements are indicated by red when the dipole is supported and by blue when levitated. **b**, During levitation, the visible light emission shows neutrals do not penetrate into the high-density central region during levitation in contrast to the emission observed with a supported dipole. **c**, High-speed measurements of the time evolution of the four line-density chords show the centrally peaked density profile is established in 25 ms. The dashed lines show the inward pinch calculated from equation (1) with D using the electric field fluctuations measured with edge probes reproduces the measured density evolution. When the microwave power is switched off, the plasma density seems to decay more quickly at the outer region during levitation and more quickly at the inner region with a supported dipole.

within flux tubes, $N = \langle n \rangle \delta V$, move as a unit. The electric field is expressed as the gradient of a potential, $E_\varphi = R^{-1} \partial \tilde{\Phi}(\psi, \phi, t)/\partial \varphi$ with R being the cylindrical radius. The fluctuating potential $\tilde{\Phi}$ does not vary along a magnetic field line but varies from field line to field line, each labelled by an azimuthal angle, ϕ, and the magnetic flux, ψ, which varies approximately as the inverse of the outer equatorial radial location of the field line, $\psi \propto 1/L$. If there are no losses along the field line, the diffusion is loss-free. Diffusion reduces gradients of flux-tube particle number, N, which leads to a centrally peaked density profile. When the radial diffusion of N is written in terms of gradients with respect to magnetic flux, then $N(\psi, t)$ evolves in time as

$$\frac{\partial N}{\partial t} = \langle S \rangle + \frac{\partial}{\partial \psi} D \frac{\partial N}{\partial \psi} \qquad (1)$$

where $\langle S \rangle$ is the net particle source within the flux tube, and the diffusion coefficient is $D = R^2 \langle E_\varphi^2 \rangle \tau_{\rm cor}$ in units of $(\mathrm{V\,s})^2\,\mathrm{s}^{-1}$. D is proportional to the product of the mean-squared fluctuations of the azimuthal electric field and the correlation time of the fluctuations[2]. When equation (1) is expressed in terms of the particle density $\langle n \rangle$, the radial particle flux is equal to $\Gamma_\psi = -D \delta V \partial \langle n \rangle / \partial \psi + V_\psi \langle n \rangle$, where $V_\psi \equiv -D\, \partial \delta V / \partial \psi$ is the turbulent pinch velocity.

We have not yet measured the structure of the plasma fluctuations in LDX, nor do we know how the convective interchange diffusion coefficient, D, varies with radius. However, we measure the potential and electric-field fluctuations at the plasma edge, and the fluctuation spectra for both the inner interferometer chord and the floating potential probes at the plasma edge are similar (as shown in Supplementary Figs S4a and S4b). The edge potential fluctuations are measured with an array of 24 floating probes, located at a radius $R = 1$ m, some of which appear at the bottom of Fig. 4b. Using these probes, the diffusion coefficient at the plasma edge is estimated to be $D \approx 0.047\,(\mathrm{V\,s})^2\,\mathrm{s}^{-1}$, using the measured values of $\langle E_\varphi \rangle \approx 54\,\mathrm{V_{r.m.s.}\,m^{-1}}$ and $\tau_{\rm cor} \approx 16\,\mu\mathrm{s}$ (shown in Supplementary Fig. S4d). This value of D is consistent with the measured time of the inward diffusion shown in Fig. 4c. Expressed in terms of an inward pinch velocity, the rapid formation of centrally peaked profiles corresponds to a turbulent pinch of $45\,\mathrm{m\,s^{-1}}$ within the plasma core and exceeds $400\,\mathrm{m\,s^{-1}}$ at the edge. (See Supplementary Information.) The dashed lines are synthetic interferometer measurements of the solution of equation (1) with $\langle S \rangle = 0$ in the closed field-line region, a fixed plasma density at the outer edge and an assumption of rapid loss to the dipole magnet at the inner edge. The agreement between the measured turbulent pinch and the solution to equation (1) implies the centrally peaked density profile observed in a levitated dipole is due entirely to cross-field interchange mixing.

Interchange mixing should also cause diffusion of the entropy density, G, and create centrally peaked pressure profiles. The entropy density is proportional to the plasma pressure, defined as $G \equiv P \delta V^\gamma$. As low-frequency $\mathbf{E} \times \mathbf{B}$ interchange motion is adiabatic, the entropy pinch is governed by an equation of the same form as equation (1), except the net particle source, $\langle S \rangle$, must be replaced by a term proportional to the net heating or energy loss (for example, radiation or charge-exchange) within a flux tube. For loss-free adiabatic convection, the adiabatic index is $\gamma \sim 5/3$, and the plasma pressure should become even more strongly peaked than the density because $P \propto 1/\delta V^\gamma$. We believe the increased ring current observed during levitation is consistent with uniform entropy density. This conclusion is motivated by the time evolution of the equilibrium magnetic field that is measured by the outer flux loop during levitation (Fig. 4a). The increased plasma ring current cannot be explained by an increase of hot-electron stored energy, because the timescales of the ring current build-up and decay are characteristic of the plasma density and not of the cyclotron emission resulting from the hot electrons.

© 2010 Macmillan Publishers Limited. All rights reserved.

For this discharge, levitation increases plasma stored energy by approximately 60 J, equivalent to an average thermal electron temperature of 160 eV (see estimation in the Supplementary Information). This result is consistent with a uniform entropy density profile having a central electron temperature of 500 eV (at an equatorial radius of 0.77 m) and an edge temperature of 15 eV, consistent with edge Langmuir probe measurements. The thermal plasma energy associated with the inward pinch comes from the injected microwave power. Although we have not measured the process by which microwave heating generates electric fluctuations, we note simulations that show central heating can excite low-frequency interchange instabilities while relaxing central pressure gradients[30,31] and that non-symmetric heating can drive electrostatic convective cells[32].

Efforts are now underway to measure the pressure profile evolution and thereby measure the adiabatic index for interchange mixing in a dipole magnetic field. If the adiabatic index proves to be $\gamma \sim 5/3$ and if plasma dynamics remain as reported here as the plasma size and density increase, then laboratory dipole confinement of hot plasma would meet necessary physics requirements for tritium-free fusion power[28,29].

Methods

Experiment. All experiments were carried out using the LDX (ref. 33), which confines high-temperature plasma in the field of a superconducting dipole magnet. The superconducting dipole is made from a single 1.5-km-long Nb_3Sn superconducting cable, wound into 716 turns at an approximate radius of 0.33 m and encapsulated inside a toroidal liquid-helium cryostat[34]. The dipole is inductively charged to $I_d = 1.12$ MA · turns and creates a dipole moment of $0.34 I_d$ A m^{-2} having an on-axis field strength of 2.1 T. A water-cooled copper magnet is located 1.53 m above the superconducting dipole. When this levitation coil is energized to 0.285 MA · turns, an upward magnetic attraction opposes the dipole's gravitational mass of 565 kg. The dipole position is monitored with an array of eight laser-position detectors, and the levitation current is adjusted with a real-time digital feedback controller capable of maintaining the dipole's position to within ±0.5 mm. The superconducting dipole magnet warms slowly, allowing more than two hours of experimentation with a levitated dipole before it must be recooled with liquid helium.

Supplementary Fig. S1 shows a schematic diagram of the LDX facility and photographs of the interior and exterior of the large, 5-m-diameter, stainless-steel plasma-containment vessel. A high-field superconducting magnet, used to inductively charge the dipole, is located below the vacuum vessel. The water-cooled copper levitation coil and a pneumatic hoist are installed on top of the vessel. After lifting the dipole magnet into position, plasma is created and confined within the vacuum vessel. Mechanical and control safeguards prevent excessive upward acceleration of the dipole towards the levitation magnet, and an array of springs, located within a light-weight 'launcher-catcher', cushion the fall of the dipole should the levitation system fail accidentally.

Creating plasma discharges confined by a levitated dipole. Plasma is created, heated and sustained by injecting up to 15 kW of microwave power using a combination of sources at 2.45, 6.4 and 10.5 GHz and injecting neutral gas, typically deuterium. The injected microwaves reflect off the vacuum vessel and are absorbed at surfaces within the plasma that resonate with harmonics of the electron cyclotron frequency[35]. The plasma parameters depend on the amount of power applied at each frequency[36]. When the neutral density is below a threshold (and is approximately 1.0 μtorr), intense HEI instabilities are excited that degrade plasma confinement[37]. At higher neutral pressure, the instabilities stabilize and plasma density increases with pressure until the pressure exceeds approximately 10 μtorr, when the plasma density is limited by the level of injected microwave power.

Plasma discharges produced within the LDX device are measured using several diagnostics in addition to those discussed in the primary text (namely, four interferometer channels, magnetic flux loops, millimetre-wave radiometers and edge electrostatic probes). These are: (1) two 16-channel high-speed photodiode arrays to allow viewing of low-order non-axisymmetric fluctuations; (2) two high-speed video cameras with frame rates that can reach over 10,000 fps; and (3) multiple X-ray spectrometers and an X-ray camera.

A movie showing a time-lapse record of the first plasma experiment using a levitated dipole is available in the Supplementary Information.

Estimating plasma parameters from measurements. The plasma density profile, the plasma stored energy, the diffusion coefficient resulting from random electric-field fluctuations and the speed of the turbulent pinch are estimated from measurements using the methods described in the Supplementary Information. The observation of the inward particle pinch and of the centrally peaked density profile requires a model-dependent inverse integral calculation using the four-channel interferometer array[38].

Received 27 August 2009; accepted 11 December 2009; published online 24 January 2010

References

1. Falthammar, C.-G. Effects of time dependent electric fields on geomagnetically trapped radiation. *J. Geophys. Res.* **70,** 2503–2516 (1965).
2. Birmingham, T. Convection electric fields and diffusion of trapped magnetospheric radiation. *J. Geophys. Res.* **74,** 2169–2181 (1969).
3. Schulz, M. & Lanzerotti, L. J. *Particle Diffusion in the Radiation Belts* (Springer, 1974).
4. Lyon, J. G. The solar wind-magnetosphere-ionosphere system. *Science* **288,** 1987–1991 (2000).
5. Northrop, T. & Teller, E. Stability of the adiabatic motion of charged particles in the Earths field. *Phys. Rev.* **117,** 215–225 (1960).
6. Rosenbluth, M. N. & Longmire, C. L. Stability of plasmas confined by magnetic fields. *Ann. Phys.* **1,** 120–140 (1957).
7. Frank, L. A. On the extraterrestrial ring current during geomagnetic storms. *J. Geophys. Res.* **72,** 3753–3767 (1967).
8. Lyons, L. R. & Williams, D. J. The storm and poststorm evolution of energetic (35–560 keV) radiation belt electron distributions. *J. Geophys. Res.* **80,** 3985–3994 (1975).
9. Lyons, L. R. & Williams, D. J. Storm-associated variations of equatorially mirroring ring current protons, 1–800 keV, at constant first adiabatic invariant. *J. Geophys. Res.* **81,** 216–220 (1976).
10. Koepke, M. Interrelated laboratory and space plasma experiments. *Rev. Geophys.* **46,** 1–43 (2008).
11. Warren, H. & Mauel, M. E. Observation of chaotic particle-transport induced by drift-resonant fluctuations in a magnetic dipole field. *Phys. Rev. Lett.* **74,** 1351–1354 (1995).
12. Levitt, B., Maslovsky, D. & Mauel, M. E. Observation of centrifugally driven interchange instabilities in a plasma confined by a magnetic dipole. *Phys. Rev. Lett.* **94,** 175002 (2005).
13. Garbet, X. *et al.* Turbulent particle transport in magnetized plasmas. *Phys. Rev. Lett.* **91,** 035001 (2003).
14. Hoang, G. T. *et al.* Parametric dependence of turbulent particle transport in tore supra plasmas. *Phys. Rev. Lett.* **93,** 135003 (2004).
15. Baker, D. A perturbative solution of the drift kinetic equation yields pinch type convective terms in the particle and energy fluxes for strong electrostatic turbulence. *Phys. Plasmas* **11,** 992–996 (2004).
16. Bourdelle, C. Turbulent particle transport in magnetized fusion plasma. *Plasma Phys. Control. Fusion* **47,** A317–A326 (2005).
17. Weiland, J., Eriksson, A., Nordman, H. & Zagorodny, A. Progress on anomalous transport in tokamaks, drift waves and nonlinear structures. *Plasma Phys. Control. Fusion* **49,** A45–A57 (2007).
18. Burch, J. L. *et al.* Views of Earth's Magnetosphere with the IMAGE Satellite. *Science* **291,** 619–624 (2001).
19. Russell, C. T. The dynamics of planetary magnetospheres. *Planet. Space Sci.* **49,** 1005–1030 (2001).
20. Yamada, T. *et al.* Anatomy of plasma turbulence. *Nature Phys.* **4,** 721–725 (2008).
21. Furth, H. P. Magnetic confinement fusion. *Science* **249,** 1522–1527 (1990).
22. Boxer, A. C., Garnier, D. T. & Mauel, M. E. Multichannel microwave interferometer for the levitated dipole experiment. *Rev. Sci. Instrum.* **80,** 043502 (2009).
23. Wolf, R. A., Spiro, R., Sazykin, S. & Toffoletto, F. How the Earth's inner magnetosphere works: an evolving picture. *J. Atmos. Solar Terr. Phys.* **69,** 288–302 (2007).
24. Melrose, D. B. Rotational effects in the magnetosphere of Jupiter. *Planet. Space Sci.* **15,** 381–393 (1967).
25. Garnier, D. T. *et al.* Production and study of high-beta plasma confined by a superconducting dipole magnet. *Phys. Plasma* **13,** 056111 (2006).
26. Hasegawa, A. A dipole field fusion reactor. *Comments Plasma Phys. Control. Fusion* **11,** 147–151 (1987).
27. Hasegawa, A., Chen, L. & Mauel, M. E. A D-^{3}He fusion-reactor based on a dipole magnetic-field. *Nucl. Fusion* **30,** 2405–2413 (1990).
28. Hoffert, M. *et al.* Advanced technology paths to global climate stability: Energy for a greenhouse planet. *Science* **298,** 981–987 (2002).
29. Kesner, J., Garnier, D. T., Hansen, A., Mauel, M. E. & Bromberg, L. Helium catalysed D–D fusion in a levitated dipole. *Nucl. Fusion* **44,** 193–203 (2004).
30. Pastukhov, V. & Chudin, N. Self-consistent turbulent convection in a magnetized plasma. *JETP Lett.* **82,** 356–365 (2005).
31. Kouznetsov, A., Freidberg, J. P. & Kesner, J. Quasilinear theory of interchange modes in a closed field line configuration. *Phys. Plasmas* **14,** 102501 (2007).
32. Kesner, J. & Garnier, D. Convective cell formation in a levitated dipole. *Phys. Plasmas* **7,** 2733–2737 (2000).

© 2010 Macmillan Publishers Limited. All rights reserved.

33. Garnier, D. T. *et al.* Design and initial operation of the LDX facility. *Fusion Eng. Des.* **81,** 2371–2380 (2006).
34. Zhukovsky, Z. *et al.* First integrated test of the superconducting magnet systems for the levitated dipole experiment (LDX). *Fusion Eng. Des.* **75,** 29–32 (2005).
35. Stix, T. H. *Waves in Plasmas* (American Institute of Physics, 1992).
36. Hansen, A. K. *et al.* Varying electron cyclotron resonance heating on the Levitated Dipole Experiment. *J. Fusion Energy* **26,** 57–60 (2007).
37. Ortiz, E. E. *et al.* Effects of the hot electron interchange instability on plasma confined in a dipolar magnetic field. *J. Fusion Energy* **26,** 139–144 (2007).
38. Boxer, A. C. *Density Profiles of Plasmas Confined by the Field of a Levitating, Dipole Magnet, Doctoral Dissertation* (MIT, 2008).

Acknowledgements

The authors acknowledge the technical expertise of R. Lations, P. Michael, J. Minervini, D. Strahan and A. Zhukovsky that has been required for the design and successful operation of the LDX superconducting magnets. LDX is a joint research project of Columbia University and the Massachusetts Institute of Technology and is supported by the USDOE Office of Fusion Energy Sciences with Grants DE-FG02-98ER54458 and DE-FG02-98ER54459.

Author contributions

A.B. constructed the interferometer array and parameterized the density profile. R.B. constructed and installed the probe array. J.E. installed and analysed optical measurements. P.W. installed and calibrated the radiometers. D.G. designed and implemented the dipole levitation system and supervised operation of the experimental facility. M.E.M. noted the time-evolution of the inward particle pinch, modelled the relationship between edge fluctuations and diffusion and drafted the article. All authors participated in the planning and execution of experiments, discussed the experimental results and commented on the manuscript.

Additional information

The authors declare no competing financial interests. Supplementary information accompanies this paper on www.nature.com/naturephysics. Reprints and permissions information is available online at http://npg.nature.com/reprintsandpermissions. Correspondence and requests for materials should be addressed to M.E.M.

© 2010 Macmillan Publishers Limited. All rights reserved.

nature physics

SUPPLEMENTARY INFORMATION

DOI: 10.1038/NPHYS1510

Turbulent Inward Pinch of Plasma Confined by a Levitated Dipole Magnet

A.C. Boxer,[1] R. Bergmann,[1] J.L. Ellsworth,[1] D.T. Garnier,[2] J. Kesner,[1] M.E. Mauel,[2*] P. Woskov[1]

1. Plasma Science and Fusion Center, Massachusetts Institute of Technology, Cambridge, Massachusetts 02139, USA.

2. Department of Applied Physics and Applied Mathematics, Columbia University, New York, New York, 10027, USA.

* e-mail: mauel@columbia.edu.

This PDF file includes:

1. Supplementary Figure S1
2. Method to estimate plasma density profile
3. Method to estimate plasma energy from magnetic flux
4. Method to estimate particle diffusion from electric field fluctuations
5. Method used to characterize turbulent pinch
6. Notes describing other relevant work
7. Legend for Movie S1
8. Supporting References

Supplementary Figure S1

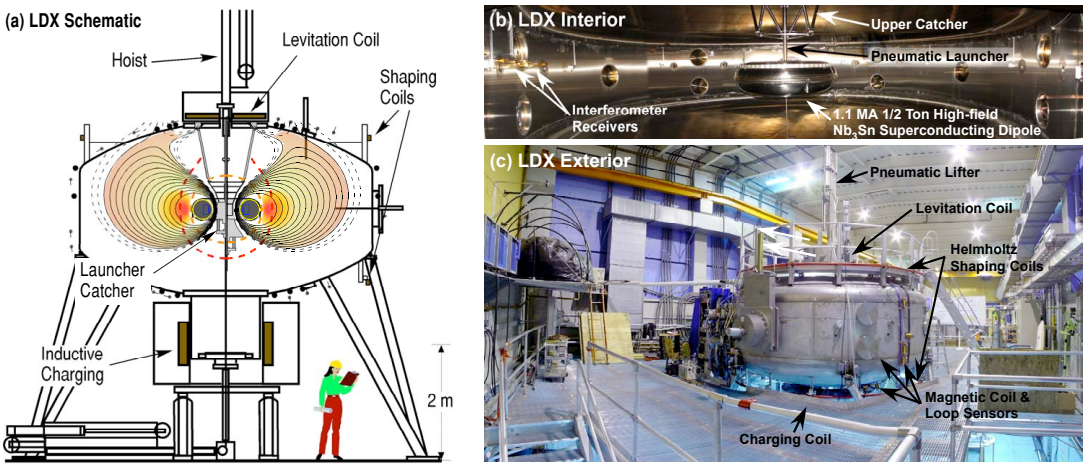

Figure S1 The Levitated Dipole Experiment (LDX). a, Schematic of the Levitated Dipole Experiment (LDX) showing the location of the superconducting dipole in the center of the 5 m vessel. Prior to experiments, the dipole is inductively charged within the lower charging coil. **b,** Photograph of the interior of the plasma discharge chamber showing the locations of the interferometer receivers. **c,** Photograph of the exterior of the experimental device, located in a large experimental hall.

Method to estimate plasma density profile.

The evolution of the plasma density profile is measured with an interferometer array consisting of four heterodyne receivers with quadrature phase detectors and one transmitting horn launching polarized 60 GHz microwaves across the plasma. The geometry of the interferometer ray paths are shown in Figs. 1a and 3a in the primary text. The measured phases are proportional to the density integrated along each path with an accuracy of approximately $\pm 5^\circ$. The phases are recorded every 2 μsec, allowing for measurement of line-density fluctuations.

The time-averaged density profile is estimated from the four phase measurements using a model-dependent inverse integral calculation described by Ref. 33 in the primary text. Assuming the density is axisymmetric, the density profile is found from the inverse Abel transform of the interferometer phase when measured as a smooth, continuous function of the ray's tangency radius.[S1] With only four chords, additional assumptions are required. Fig. S2 shows the profiles calculated using three such methods. In the first method, the particle content, N, within tubes of given magnetic flux is assumed to be piece-wise discontinuous but constant within the four annular sections defined by the interferometer

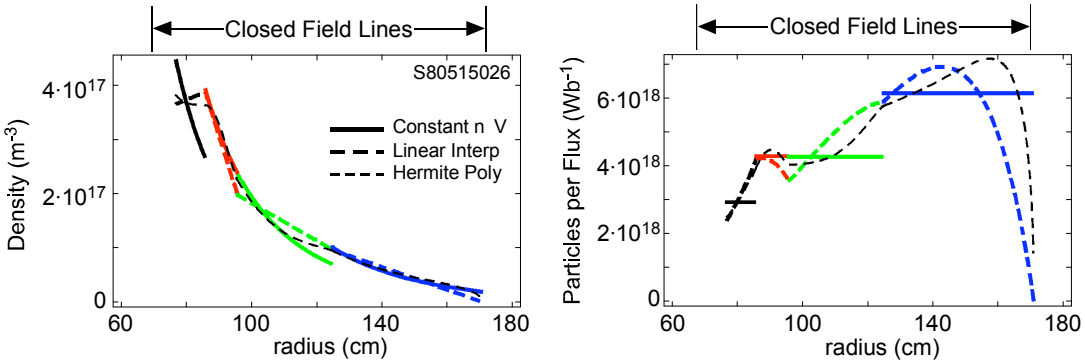

Figure S2 Example of the time-averaged density and particle number profiles for a discharge with a levitated dipole estimated using three methods. The measured interferometer phases (radians) averaged over the period from 4 to 8 sec were $8.08 \pm 4.2\%$, $6.71 \pm 3.9\%$, $4.51 \pm 4.6\%$, and $2.04 \pm 16\%$. **a,** The time-averaged density profile, $\langle n \rangle$. **b,** The equivalent profile when expressed as flux-tube particle number, N.

chords, shaded with different colors in Fig. 3a. The density is taken to be uniform along a magnetic field-line, so the equatorial density is related to the particle number as $\langle n \rangle = N/\delta V$, where the differential volume of a tube of magnetic flux is $\delta V = \oint ds/B \sim L^4$. In the second method, the plasma density, $\langle n \rangle$, is taken to be piece-wise continuous and to vary linearly within each of the four annular regions, producing a plasma density profile that is linearly interpolated between the ray path's tangency radii. In the third method, a smooth function of the interferometer phase with radius is first constructed using Hermite polynomial interpolation, and the plasma density profile is then computed using the inverse Abel transform. As shown in Fig. S2, all three methods produce similar estimates for the plasma density profile, and they are sufficient to establish the central peaking of the plasma density during levitation of the dipole magnet. We have assumed the density to be constant along field lines as is observed fusion experiments when field lines trace out flux surfaces.

Method to estimate plasma energy from magnetic flux.

The equilibrium diamagnetic current of the plasma is related to the gradient of the plasma pressure, and we use measurements of the magnetic field and flux from the plasma's "ring current" to estimate the confined plasma kinetic energy.[S2] The relationship between the plasma energy confined in the Earth's magnetosphere and the magnetic field strength at the surface of the Earth's equator is known as the Dessler-Parker-Sckopke relation.[S3, S4, S5] Measurement of the plasma pressure in magnetic fusion confinement devices is based on a reconstruction of equilibrium plasma profiles that determine the plasma toroidal current

density using a least-squares method.[S6]

Estimates of the plasma energy in LDX are based on these two methods: (i) least-squares reconstruction of the plasma ring current density parameterized by a model pressure profile and (ii) computation of the relationship between the magnetic flux measured at the outer equator of the plasma containment vessel. We find magnetic reconstruction of the plasma pressure profile needs to be augmented with additional measurements that constrain the radial location of the pressure because the majority of LDX magnetic diagnostics are far from the plasma. Although it is difficult to determine the plasma pressure profile magnetically, the total plasma energy (proportional to the integral of the plasma pressure) is approximately linearly related to the measured outer flux over a wide range of reasonable plasma pressure profiles. This relationship is analogous to the Dessler-Parker-Sckopke relation, making the outer flux loop a useful estimator for total plasma energy.

As described in Refs.,[S2,S5] the plasma toroidal current density is given by

$$\begin{aligned} J_\phi &= \hat{\phi} \cdot \frac{\mathbf{B}}{B^2} \times \left(\nabla P_\perp + \frac{P_{||} - P_\perp}{B^2} (\mathbf{B} \cdot \nabla) \mathbf{B} \right) \\ &= r \left[D_\psi P_\perp + 2p P_\perp D_\psi \ln B/(1+2p) \right] , \end{aligned}$$

where $P_\perp$ is the pressure perpendicular to the magnetic field, and $P_{||}$ is the pressure parallel to the magnetic field. The dipole magnetic field is expressed in terms of the magnetic flux, $\mathbf{B} = \nabla\phi \times \nabla\psi$, and the total flux measured by the outer flux-loop is $2\pi\psi$ at the loop location. In our calculations, we use an isotropic pressure profile that was used to study plasma stability in the magnetic field of a point-dipole,[S7] with the parallel and perpendicular pressure profiles taken to be proportional, $P_\perp/P_{||} = 1 + 2p$. In general, the equilibrium perpendicular plasma pressure depends only upon the magnetic flux, ψ, and the magnitude of the magnetic field strength, B. A two-parameter model for the pressure profile is $P_\perp(\psi, B) = P_0\, h(\psi)(\psi/\psi_0)^{4g}\, (B_0(\psi)/B)^{2p}$ where $B_0(\psi)$ is the minimum field strength along a field-line and $h(\psi)$ is a function chosen to vanish at the outer surface of the superconducting dipole and to equal unity at the plasma pressure peak at $\psi = \psi_0$. The gradient of the plasma pressure is defined in terms of the magnetic flux as $D_\psi \equiv |\nabla\psi|^{-2} \nabla\psi \cdot \nabla$. The steepness of the plasma pressure profile is set by the parameter g. An isotropic pressure profile is predicted to be marginally stable to pressure-driven interchange instabilities when $g \sim 5/3$, corresponding to a centrally-peaked pressure profile with steep radial gradients $P \sim 1/L^{20/3}$. Discharges with a fraction of hot electrons can have stable profiles with $g > 5/3$ because gyrokinetic effects give the hot electron interchange instability a real frequency that allows ion polarization currents to stabilize steep pressure gradients. We find anisotropic profiles with steep gradients produce the least-squares best fit to magnetic measurements in stable, long-pulse discharges made with a supported dipole and dominated by hot electron pressure.[S2]

Fig. S3 shows the calculated ratios of the total plasma energy to the plasma ring-current, W_E/I_p, and to the magnetic flux, W_E/Ψ, detected at the outer flux loop. The

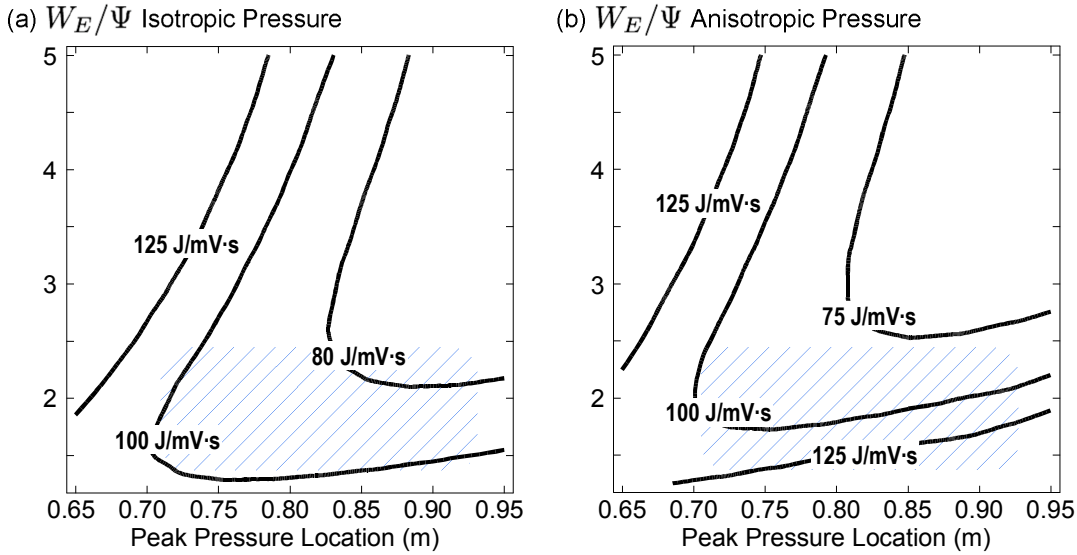

Figure S3 Calculated relationship between the plasma stored energy and the outer flux loop for a plasma pressure profile parameterized by two parameters: the radial location of the pressure peak and the profile steepness parameter, g. a, The ratio of the stored energy to the measured flux for an isotropic ($P_\perp \sim P_{||}$) pressure profile appropriate for thermal plasma confined by a levitated dipole. **b,** The ratio for an anisotropic ($P_\perp \sim 3P_{||}$) pressure profile appropriate for discharges with a supported dipole. The expected pressure parameters are indicated by color cross-hatching that defines the outer flux loop as a plasma energy estimator as $W_E/\Psi \approx 80 - 100$ J/mV·sec.

calculated flux-loop measurement is from a full plasma equilibrium including the effect due to the reduction of the current in the superconducting dipole induced by the plasma current.[S2] Based on x-ray imaging of discharges produced with a supported dipole, we expect the pressure peak to be located between 0.7 m and 0.9 m, a region encompassing the innermost closed field-line and the equatorial fundamental cyclotron resonances. Although discharges created with a supported dipole that contained trapped hot electrons were anisotropic ($P_\perp/P_{||} \sim 5$) with steep pressure profiles, $g \sim 2.8 > 5/3$, we expect the thermal plasma confined by a levitated dipole to have an isotropic pressure profile with a gradient near, or slightly steeper than, marginal stability, $g \sim 5/3$. Fig. S3 indicates how we estimate the plasma energy from outer flux loop measurements. For example, an isotropic plasma near marginal stability with 100 J of plasma energy produces produces approximately 1.1 mV·sec of flux ($W_E/\Psi \approx 90$ J/mV·sec). Equilibrium calculations show this flux measurement corresponds to approximately 1 kA of plasma ring current ($W_E/I_p \approx 100$ J/kA.) The measurement does not depend strongly insensitive to upon the anisotropy of the plasma pressure.

With the total energy estimated by the outer flux-loop and the particle number mea-

sured with the interferometer array, the average plasma temperature can also be estimated. The plasma volume is $2\pi \int d\psi \delta V = 10$ m^3, and the total number of particles is $2\pi \int d\psi N$. Using these measurements, the average electron temperature is $\langle T \rangle \approx W_e/(3\pi \int d\psi N)$. For the levitated discharge illustrated by Fig. 4 in the primary text, we estimate the thermal plasma energy to be 60 J. The interferometer measurement implies the average temperature is 160 eV. Because microwave heating is applied directly to plasma electrons and because the plasma density is relatively low, we believe the electron temperature significantly exceeds the ion temperature. This assumption is consistent with characteristic collision frequencies. With $\langle T \rangle \approx \langle T_e \rangle \approx 160$ eV, the thermal electrons are collisionless since the mean-free-path is many times longer than the length along the magnetic field. The product of the thermal electron bounce frequency and the collision frequency, $\omega_{be}\tau_e$, exceeds 10^3 throughout most of the plasma profile. Because the plasma density is low, the time-scale for collisional thermal relaxation between the thermal electrons and cold ions is of the order of one-half second. Since this is much longer than the particle confinement time, the electron and ion temperatures decouple. Although electron dynamics are collisionless along magnetic field lines, the period of the electrostatic turbulence (dominated by frequencies of the order of 1 kHz, as indicated in Fig. 4c) that cause cross-field transport are comparable to the electron collision time. The electron collision frequency ranges from 0.1 msec at the edge to 0.8 msec centrally. This implies that the thermal electron velocity distribution remains nearly Maxwellian during the slow cross-field motion of the turbulent pinch, a condition referred to as "semi-collisional" with regards to interchange dynamics.[S8]

We have not yet measured the plasma pressure profiles, but theoretical considerations (referenced in the primary text) imply that interchange turbulence drives the profiles towards marginally stablity. A mariginally stable pressure has entropy density $G = P\delta V^\gamma$ that is independent of radius within the volume of closed field-lines. With this assumption, the electron temperature profile can be calculated from the plasma energy measured from the flux loop and the measured density profile.

For a marginally stable pressure profile having an ideal adiabatic index, $g \sim \gamma \sim 5/3$, the temperature at the tangency radius of the inner interferometer chord (0.77 m) reaches 500 eV, while the temperature at the outer edge is approximately 15 eV, consistent with measurements using edge Langmuir probes. Direct measurement of the thermal plasma profile is presently an active research project that will determine the adiabatic index for plasma interchange mixing in a dipole magnetic field.

Method to estimate particle diffusion from electric field fluctuations.

We estimate the particle diffusion coefficient due to random $\mathbf{E}\times\mathbf{B}$ plasma motion by measuring the time-averaged cross-correlation of the azimuthal gradient of the electrostatic

potential with an array of 24 floating potential probes. The probes are located at the plasma edge (and shown at the lower part of Fig. 4b in the primary text) at a radius of $R = 1$ m, equally spaced in azimuth, and spanning a 90-degree sector ($\Delta\varphi = \pi/46 \approx 4°$). The azimuthal electric field is estimated from the floating potential difference between adjacent probes, $E_\varphi \approx (\Phi(\varphi + \Delta\varphi) - \Phi(\varphi))/R\Delta\varphi$. The radial $\mathbf{E} \times \mathbf{B}$ velocity of the plasma due to interchange fluctuations is $V_\psi \equiv \dot{\psi} = RE_\phi$, in units of V·sec/sec. If the electric potential fluctuations are random, then the particle diffusion coefficient is $D = R^2\langle E_\varphi^2\rangle\tau_c$ when expressed in units appropriate to Eq. 1 in the primary text (*i.e.* $(\text{V·sec})^2/\text{sec}$). D is equal to the product of the mean squared radial velocity and the autocorrelation time. For the discharges reported here, the amplitude of auto-correlation decays exponentially with time lag, and we compute the correlation time by integrating the normalized auto-correlation, $\tau_c \equiv \langle E_\varphi^2\rangle^{-1} \int_0^\infty d\tau \langle E_\varphi(\tau)E_\varphi(0)\rangle$.

Fig. S4 shows the averaged fluctuation spectra and normalized cross-correlations measured for both the supported and levitated discharges shown in Fig. 4 in the primary text. The spectra and correlation functions were averaged from 5.10 to 5.49 sec using 200 overlapping intervals 4 msec long. The fluctuations of both the edge floating potential and the interferometer have maximum intensity near 600 Hz, and the power spectra decreases with frequency according to an inverse power-law. The measured correlation time for electric field fluctuations is approximately 16 μsec, but the floating potential and line-density fluctuations have a correlation time more than twice as long. Fig. S4 also shows the cross-correlation between probes along the probe array and between the interferometer chords. The azimuthal correlation length of the floating potential is ~ 0.3 m. The fluctuations are similar whether or not the dipole is levitated, and this observation indicates that the processes that determine the fluctuation intensity do not depend strongly on either parallel losses or plasma profiles.

Modeling the plasma diffusion using Eq. 1 requires knowledge of the net particle source or loss, $\langle S\rangle$, and the diffusion coefficient, D, across the plasma radius. Visible photography (like Fig. 4b in the primary text) suggest that the particle source peaks at the outer edge during levitation; however, discharge-to-discharge variation in the inner density suggest the net particle source or loss at the surface of the superconducting dipole can vary depending upon surface conditioning that changes surface-adsorbed gas. We are still in the process of measuring the structure of the plasma fluctuations in LDX; however, detailed plasma fluctuations observed with other mechanically-supported dipoles[S9,S10] and with nonlinear computer simulations[S11] show fluctuations that are dominated by long azimuthal and radial structures. These related observations and the similarity between the line-density and probe fluctuations are compatible with the assumption that azimuthal structure and the mean-squared potential fluctuations are uniform with radius. This condition makes D uniform across the plasma radius. It corresponds to a fluctuating electric field that increases with decreasing radius, $\langle E_\varphi^2\rangle \sim R^{-2}$. Since the fluctuations are steady in time, so is D. With the diffusion coefficient uniform and equal to the value estimated with the edge probe array, $D \sim 0.047$ $(\text{V·msec})^2/\text{msec}$, we can find a solution

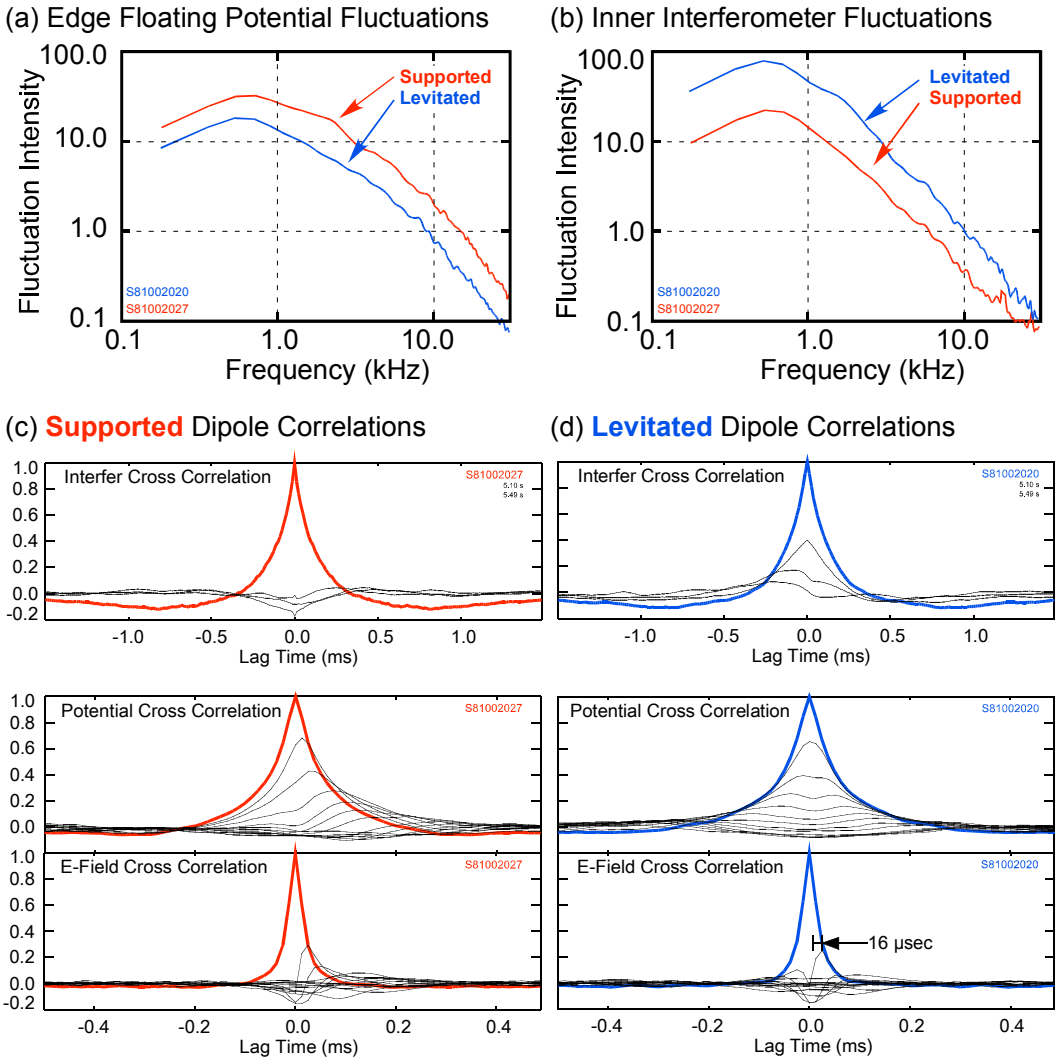

Figure S4 The average frequency spectrum and average cross correlations of probe and interferometer measurements. a, The floating potential fluctuation intensity measured using Langmuir probes at the plasma edge (in units of V^2/kHz^2). **b,** The fluctuations of the central line-density (in units of $radian^2/kHz^2$). **c,** The normalized cross and auto-correlations of the interferometer array and of the edge potential probes are shown for the supported discharge discussed in the primary text and shown in Fig. 4. **d,** The average correlations for the equivalent levitated levitated discharge. The correlation time of the electric field fluctuations is approximately 16 μsec. The characteristics of plasma fluctuations are similar whether or not the dipole is levitated.

of Eq. 1 that reproduces the time-scale and general features of the observed build-up of centrally peaked plasma density (Fig. 4c). The synthetic line-density measurements shown in Fig. 4c were computed from a solution to Eq. 1 using simple boundary conditions: the plasma density at the outer edge is constant and the plasma density vanishes at the surface of the dipole magnet. The modeled line-density reproduces the 25 msec time-scale for the development of the centrally peaked profile; however, temporal deviations exist between the simple diffusion model and the measured density profile evolution. We believe these temporal deviations result from time variation of the net particle source, $\langle S \rangle$, and from the presence of large-scale, quasi-coherent (and possibility intermittent) convection that is not represented by the quasilinear model for radial diffusion.[S12,S13]

Method used to characterize turbulent pinch

Plasma compressibility creates a turbulent particle pinch from low-frequency electrostatic turbulent transport. The role of compressibility can be made explicit by deriving Eq. 1 (in the primary text) from the flux-tube integral of a local continuity equation containing both cross-field diffusive and radial pinch terms. The radial particle flux is $\mathbf{\Gamma} = -\mathsf{D}_{rr} \cdot \nabla\langle n \rangle + \mathbf{V}_r \langle n \rangle$. Noting that the plasma density and flux-tube particle number are related by $\langle n \rangle = N/\delta V$, Eq. 1 is equivalent to the flux-tube integral of the local continuity equation

$$\begin{aligned} \frac{\partial N}{\partial t} = \delta V \frac{\partial \langle n \rangle}{\partial t} &= \langle S \rangle + \frac{\partial}{\partial \psi} \oint \frac{ds}{B} \left[D_{rr} |\nabla \psi|^2 \frac{\partial \langle n \rangle}{\partial \psi} - \nabla \psi \cdot \mathbf{V}_r \langle n \rangle \right] \\ &= \langle S \rangle + \frac{\partial}{\partial \psi} \left[D \delta V \frac{\partial \langle n \rangle}{\partial \psi} - V_\psi \langle n \rangle \right] , \end{aligned}$$

where D_{rr} is the local cross-field diffusion in units of $\mathrm{m}^2/\mathrm{sec}$ and $\mathbf{V}_r$ is the turbulent pinch in m/sec. The interchange mixing of flux-tubes, defined by Eq. 1, defines the relationship between diffusion in flux-coordinates and the equivalent radial diffusion and pinch velocity. The pinch velocity is $\nabla\psi \cdot \mathbf{V}_r = V_\psi = D\, \partial \delta V / \partial \psi$, and the diffusion coefficient is $D\delta V = \oint (ds/B) D_{rr} |\nabla \psi|^2$. Turbulent diffusion, $D\delta V$, flattens density gradients, while V_ψ is directed towards decreasing δV and causes central peaking. The net particle flux vanishes when $\partial(\langle n \rangle \delta V)/\partial \psi \to 0$, reflecting the combined action of spatial diffusion and the inward pinch of interchange turbulence. Note: D does not by itself determine global particle confinement. Instead, it is the product of D with the particle number gradient, $\partial N/\partial \psi$, and the edge boundary conditions that determines confinement. Magnetic configurations with large compressibility may have centrally-peaked $\langle n \rangle$ profiles with a vanishing gradient of N and small net particle flux.

For the dipole magnetic geometry, the flux-tube integrals give $D \approx 0.75 D_{rr} L^2 B_0^2$. The measured diffusion coefficient reported in this article, $D = 0.047$ $(\mathrm{V \cdot sec})^2/\mathrm{sec}$ is equivalent to $D_{rr} \approx 8.4$ $\mathrm{m}^2/\mathrm{sec}$ at $L = 0.77$ m. With D uniform, $D_{rr} \propto L^4$ increases

rapidly with increasing radius, which corresponds to turbulent $\mathbf{E} \times \mathbf{B}$ motion induced by a spatially uniform intensity of electrostatic potential fluctuations. The corresponding inward turbulent pinch is $V_r \approx -45$ m/sec at $L = 0.77$ m, and the magnitude of inward pinch velocity increases with radius as $V_r \propto L^3$.

Notes describing other relevant work

This research is related to efforts to (i) model large-scale dynamics of plasma trapped within planetary magnetospheres, (ii) understand turbulent transport of magnetized plasma induced by low-frequency interchange fluctuations, and (iii) use magnetic fields to confine high-temperature plasma in order to produce useful quantities of thermonuclear energy.

Magnetospheric density evolves in response to fluctuations driven by the solar wind. In contrast, the electric field fluctuations in the LDX device are self-generated and sustained by microwave heating. Although the source of fluctuations differ, the LDX fluctuations are analogous to the driven fluctuations in the Earth's cross-tail electric field that lead to ring-current energization,[S14,S15] plasmaspheric density structure and dynamics,[S16] and the dynamics of plasma density evolution in the outer planets.[S17] Although the convective processes that underlie electric field-driven diffusion in the laboratory are the same as those in the magnetosphere, the resulting diffusion coefficients vary differently with radius. In the Earth's magnetosphere, $D \sim L^2$ since the amplitude of the cross-tail electric field does not vary strongly with radius. In contrast, we measure the diffusion coefficient in the laboratory to be relatively uniform, and this implies turbulent electrostatic potential fluctuations in LDX exist throughout the plasma with comparable intensity.

Fluctuations in magnetized high-temperature plasma represent collective dynamics that significantly accelerate transport and involve nonlinear energy transfer between scales. Turbulent transport of plasma confined in a dipole field is especially revealing because the dipole geometry has large plasma compressibility without magnetic shear. The absence of magnetic shear allows nonlinear processes to cascade turbulent fluctuations to the system size.[S18,S10] Plasma compressibility makes the plasma diamagnetic drifts comparable to magnetic drifts for centrally-peaked marginally stable profiles.[S19]

We observe the turbulent pinch, V_ψ, to be large for the dipole magnetic field, since $\partial \delta V / \partial \psi$ is large. Evidence for a smaller inward pinch has been reported previously in tokamak magnetic geometry which has smaller compressibility effects.[S20,S21] Understanding the turbulent particle pinch is a major goal of magnetic confinement fusion research.[S22,S23,S24]

Because the geometry of the magnetic field determines confinement properties of plasma (*e.g.* transport and density profiles), these results contribute to efforts to produce useful quantities of thermonuclear energy through magnetic confinement of high-temperature plasma. Internal rings were used previously to study plasma confinement for this purpose[S25,S26,S27,S28,S29] since internal rings provide stable, steady confinement and

allow testing a variety of magnetic configurations. The levitated dipole geometry is different from these earlier experiments because the dipole geometry achieves larger plasma compressibility. A dipole fusion energy source would require a large, superconducting dipole,[S30] but rapid particle convection induced by electric potential fluctuations may be sufficient to extract tritons from helium-3 catalyzed deuterium fusion and make possible conditions for fusion energy without fast neutrons.[S31]

Legend for Movie S1

Movie S1 is a time-lapse record of the first plasma experiment using a levitated dipole (recorded on November 8, 2007). The movie is 1.34 min long and shows the entire sequence of events that occur during experiments with a superconducting levitated dipole. The pneumatic lifting of the dipole to and from the charging station, where the dipole is reconnected with sensors and cryogenic services, is time-lapsed five-fold.

Six frames from this movie are shown in Fig. S5. Once energized, the dipole magnet is lifted to the center of the vacuum vessel, and the levitation magnetic is switched on. Laser occultation sensors detect the position of the dipole. The pneumatic lifting apparatus is withdrawn 0.22 m, and up to three hours of plasma experiments are conducted. When experiments are completed, the spring-loaded "catcher" is elevated and re-inserted into the bore of the dipole. The levitation field is turned-off, and the dipole is returned to the charging station.

Since this first experiment, over 150,000 seconds of data have been recorded from plasma experiments with a levitated dipole.

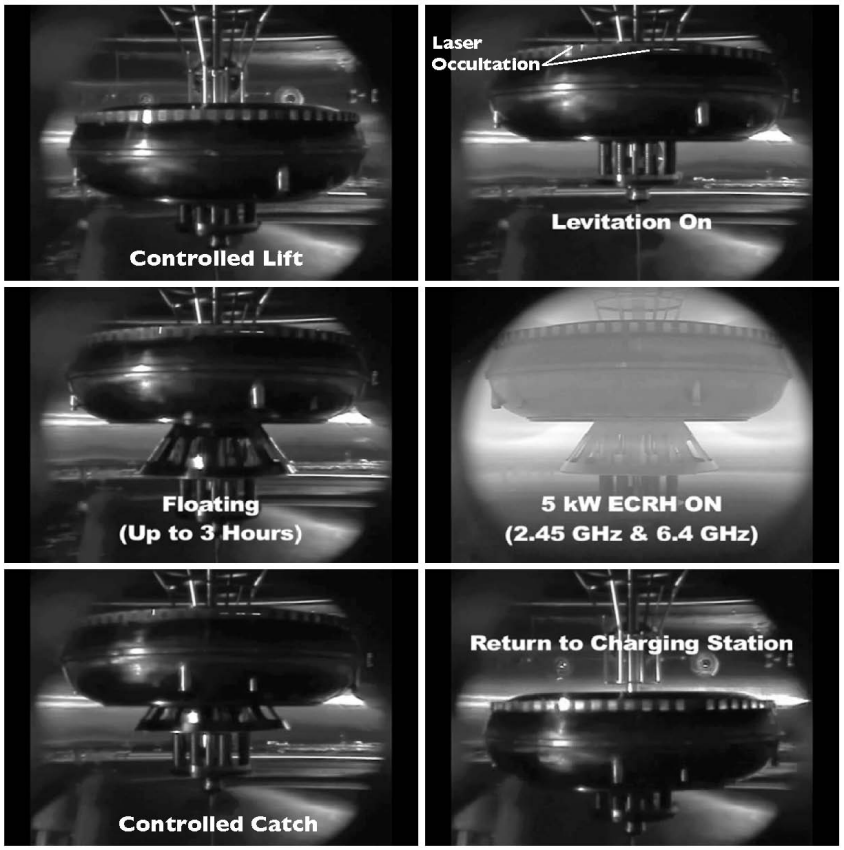

Figure S5 Frames from the attached MPEG movie showing the first levitation of the superconducting dipole magnet in November, 2007. The sequence proceeds from left to right and from top to bottom.

Supporting References

[S1] Bracewell, R., *The Fourier Transform and its Applications*, (McGraw Hill, New York, 1965).

[S2] Karim, I., *et al.*, Equilibrium reconstruction of anisotropic pressure profile in the levitated dipole experiment, *J. Fusion Energy*, **26**, 99-102 (2007).

[S3] Dessler, A.J. & Parker, E., Hydromagnetic theory of geomagnetic storms, *J. Geophys. Res.*, **64**, 2239-2252 (1959)

[S4] Sckopke, N., A general relation between the energy of trapped particles and the disturbance field near the Earth, *J. Geophys. Res.*, **71**, 3125-3130 (1966).

[S5] Daglis, I.A., Thorne, R.M., Baumjohann, W., & Orsini, S., The terrestrial ring current: Origin, formation, and decay, *Rev. Geophys.*, **37**, 407-438 (1999).

[S6] Lao, L.L., John, H.S., Stambaugh, R., & Kellman, A., Reconstruction of current profile parameters and plasma shapes in tokamaks, *Nuc. Fusion*, **25**, 1611-1622 (1985).

[S7] Simakov, A.N., Hastie, R.J., & Catto, P.J., Anisotropic pressure stability of a plasma confined in a dipole magnetic field, *Phys. Plasmas*, **7**, 3309-3318 (2000).

[S8] Kesner, J. and Hastie, R.J., Electrostatic drift modes in a closed field line configuration, *Phys Plasmas*, **9**, 395-400 (2002).

[S9] Levitt, B., Maslovsky, D., & Mauel, M.E., Measurement of the global structure of interchange modes driven by energetic electrons trapped in a magnetic dipole, *Phys. Plasmas*, **9**, 2507-2517 (2002).

[S10] Grierson, B., Worstell, M., & Mauel, M.E., Global and local characterization of turbulent and chaotic structures in a dipole-confined plasma, *Phys. Plasmas*, **16**, 055902 (2009).

[S11] Pastukhov, V.P. & Chudin, N., Plasma convection near the threshold for mhd instability in nonparaxial magnetic confinement systems, *Plasma Physics Reports*, **27**, 963-977 (2001).

[S12] Riley, P. & Wolf, R.A., Comparison of diffusion and particle drift descriptions of radial transport in the Earth's inner magnetosphere, *J. Geophys. Res.*, **97** 16865-16876 (1992).

[S13] Warren, H., *et al.*, Observation of wave-induced chaotic radial transport in a laboratory terrella experiment, *Phys. Plasmas*, **3**, 2143-2148 (1996).

[S14] Chen, M.W., Lyons, L.R., & Schulz, M., Simulations of phase space distributions of storm time proton ring current, *J Geophys Res*, **99**, 5745-5799 (1994).

[S15] Brautigam, D., *et al.*, CRRES electric field power spectra and radial diffusion coefficients, *J. Geophys. Res.*, **110**, A02214 (1-15) (2005).

[S16] Darrouzet, F., *et al.*, Plasmaspheric density structures and dynamics: properties observed by the CLUSTER and IMAGE missions, *Space Sci. Rev.*, 55-106 (2009).

[S17] Russell, C.T., Outer planet magnetospheres: a tutorial, *Adv. Space Res.*, **33**, 2004-2020 (2004).

[S18] Horton, W., Drift waves and transport, *Rev. Mod. Phys.*, **71**, 735-778 (1999).

[S19] Kesner, J., Interchange modes in a collisional plasma, *Phys. Plasmas*, **7**, 3837-3840 (2000).

[S20] Isichenko, M., Gruzinov, A., & Diamond, P.H., Invariant measure and turbulent pinch in tokamaks, *Phys. Rev. Lett.*, **74**, 4436-4439 (1995).

[S21] Baker, D., Use of the drift kinetic equation to describe electrostatic turbulent transport, *Phys. Plasmas*, **9**, 2675-2883 (2002)

[S22] Weiland, J., Eriksson, A., Nordman, H., & Zagorodny, A., Progress on anomalous transport in tokamaks, drift waves, and nonlinear structures, *Plasma Phys. Control. Fusion*, **49**, A45-A57 (2007).

[S23] Doyle, E.J., *et al.*, Chapter 2: Plasma confinement and transport, in *Progress in the ITER Physics Basis*, *Nuc. Fusion*, **47**, S18-S127 (2007).

[S24] Angioni, C., *et al.*, Particle pinch and collisionality in gyrokinetic simulations of tokamak plasma turbulence, *Phys Plasmas*, **16**, 060702 (2009).

[S25] Lehnert, B., On the possibilities of ring-current configurations as a fusion device, *Plasma Physics*, **10**, 263-279 (1968).

[S26] Freeman, R.L., *et al.*, Confinement properties of the levitated spherator, *Phys. Rev. Lett.*, **26**, 356-360, (1971).

[S27] Okabayashi, M.. Ripin, B., Schmidt, J., & Yoshikawa, S., Confinement properties in levitated spherator, *Phys. Fluids*, **16**, 2339-2345, (1973).

[S28] Drake, J.R., Greenwood, J.R., Navratil, G.A., & Post, R.S., Diffusion coefficient scaling in the Wisconsin levitated octupole, *Phys. Fluids*, **20**, 148-155, (1977).

[S29] Ferron, J., Wong, A., Dimonte, G., & Leikind, B., Interchange stability of an axisymmetric, average minimum-B magnetic mirror, *Phys. Fluids*, **26**, 2227-2233, (1983).

[S30] Teller, E., Glass, A., Fowler, T.K., Space propulsion by fusion in a magnetic dipole, *Fusion Technology*, **22**, 82-87 (1992).

[S31] Nevins, W.M., A review of confinement requirements for advanced fuels, *J. Fusion Energy*, **17**, 25-32 (1998).